



HAL
open science

Conductive thermal diode based on two phase-change materials

Suraju Olawale Kasali, Jose Ordonez-Miranda, Karl Joulain

► **To cite this version:**

Suraju Olawale Kasali, Jose Ordonez-Miranda, Karl Joulain. Conductive thermal diode based on two phase-change materials. *International Journal of Thermal Sciences*, 2020, 153, 10.1016/j.ijthermalsci.2020.106393 . hal-03017600

HAL Id: hal-03017600

<https://hal.science/hal-03017600>

Submitted on 21 Nov 2020

HAL is a multi-disciplinary open access archive for the deposit and dissemination of scientific research documents, whether they are published or not. The documents may come from teaching and research institutions in France or abroad, or from public or private research centers.

L'archive ouverte pluridisciplinaire **HAL**, est destinée au dépôt et à la diffusion de documents scientifiques de niveau recherche, publiés ou non, émanant des établissements d'enseignement et de recherche français ou étrangers, des laboratoires publics ou privés.

Conductive thermal diode based on two phase-change materials

Suraju Olawale Kasali¹

¹*Institut Pprime, CNRS, Université de Poitiers, ISAE-ENSMA, F-86962 Futuroscope Chasseneuil, France*

²*Department of Physics/Geology/Geophysics, Alex Ekwueme Federal University Ndufu-Alike Ikwo, Ebonyi State, Nigeria*

Jose Ordonez-Miranda^{1,}*

¹*Institut Pprime, CNRS, Université de Poitiers, ISAE-ENSMA, F-86962 Futuroscope Chasseneuil, France*

Karl Joulain¹

¹*Institut Pprime, CNRS, Université de Poitiers, ISAE-ENSMA, F-86962 Futuroscope Chasseneuil, France*

Abstract

The thermal rectification of a conductive thermal diode made up of two phase-change materials, whose thermal conductivities significantly change within a narrow interval of temperatures, is theoretically studied and optimized. This is done by deriving analytical expressions for the temperature profiles, heat fluxes and rectification factor. An optimal rectification factor of 60% is obtained for a thermal diode operating with terminals of VO₂ and Polyethylene with a temperature difference of 250 K spanning the metal-insulator transition of both materials. It is shown that this high rectification of a conductive thermal diode could be maximized even more by increasing the thermal conductivity variations of both diode terminals. The obtained results can thus be useful to guide the development of phase-change materials capable of optimizing the rectification of conductive heat fluxes.

Keywords: Thermal rectification, conductive thermal diode, phase-change materials.

1. INTRODUCTION

Thermal diodes allowing the heat exchange between two terminals in a given direction and blocking it in the opposite one, have attracted significant attention over the past decade, due to their potential applications in heat control [1, 2, 3]. This thermal rectification is analogous to the electrical one driven by electronic diodes and has been studied through thermal diodes operating with photons [4, 5, 6, 7], phonons [8, 9, 10, 11, 3], electrons [12] and quantum structures [13, 14]. This phenomenon was first experimentally observed by Starr [15] at the interface between copper/cuprous oxide and then observed in carbon nanotubes structures [16, 17], dielectric quantum dots [18], phase-change materials (PCMs) [19, 20, 21, 22] and bulk materials [23].

*Corresponding Author

Email address: jose.ordonez@cnrs.pprime.fr (Jose Ordonez-Miranda)

Thermal rectification of conductive heat fluxes is generally generated by the temperature dependence of the thermal conductivities of the diode terminals [24] and therefore it can, in principle, be achieved with arbitrary solid materials subjected to a sufficiently large temperature gradient. Based on the Fourier's law of heat conduction, Yang *et al.* [25] modeled and optimized the rectification ratio of a conductive thermal diode made up of two terminals, whose thermal conductivities follow either a linear or a quadratic dependence on temperature. For the linear variation, they obtained a maximum rectification ratio of 0.5, which increases to 0.86, for the quadratic dependence. These relatively high rectification ratios required a temperature difference greater than 100 K between the diode terminals, which could be difficult and expensive to achieve in practice. This drawback can be overcome by means of PCMs, such as vanadium dioxide (VO₂), nitinol, and polyethylene (PE), whose thermal conductivities strongly change in a relatively narrow interval of temperatures [26, 27, 28, 29, 30, 31, 32]. These PCMs with a strong phonon-electron correlation have recently attracted a lot of experimental and theoretical interest, due to their metal-insulator transition (MIT) at temperatures close to room temperature. For instance, the thermal conductivities of VO₂ and PE typically change within a relatively small ranges of temperature $340 \text{ K} < T < 345 \text{ K}$ and $395 \text{ K} < T < 400 \text{ K}$, respectively [33, 34]. The fact that the MIT of VO₂ occurs in a temperature range of only 5 K has motivated its application in combination with a non-PCM, as the terminal of a conductive thermal diode, however, the maximal rectification factor obtained was lower ($\sim 20\%$) [34] than that reported by Yang *et al.* [25] This indicates that the operation of a conductive thermal diode with both terminals made up of PCMs could enable not only to maximize its rectification factor, but also to reduce the temperature difference between its terminals, as was recently proposed [35]. Based on an alternative definition of the rectification factor, Hyungmook *et al.* [36] recently determined a rectification factor of 147% for a thermal diode with the terminals of VO₂ and PE, whose thermal conductivities significantly change with temperatures. This relatively high rectification was obtained by describing the thermal conductivities of both PCMs as step functions, which is similar but not equal to their real behaviors, as the phase transitions of VO₂ and PE occur in a temperature interval greater than 5 K. Therefore, a more realistic description of the thermal conductivities of the rectification of thermal diodes based on two PCMs is thus required.

In this work, we theoretically study the optimization of the rectification factor of a conductive thermal diode made up of a junction of VO₂ and PE. This is done by taking into account the temperature dependence of the thermal conductivities of these PCMs within their phase transitions. Simple analytical expressions for the temperature profiles, heat fluxes and optimal rectification factor are derived and analyzed for the steady-state heat conduction. The present study is thus based on the combination of two PCMs, which are expected to yield higher rectification factors than a thermal diode based on a single PCM, which we addressed in a previous work *et al.* [34].

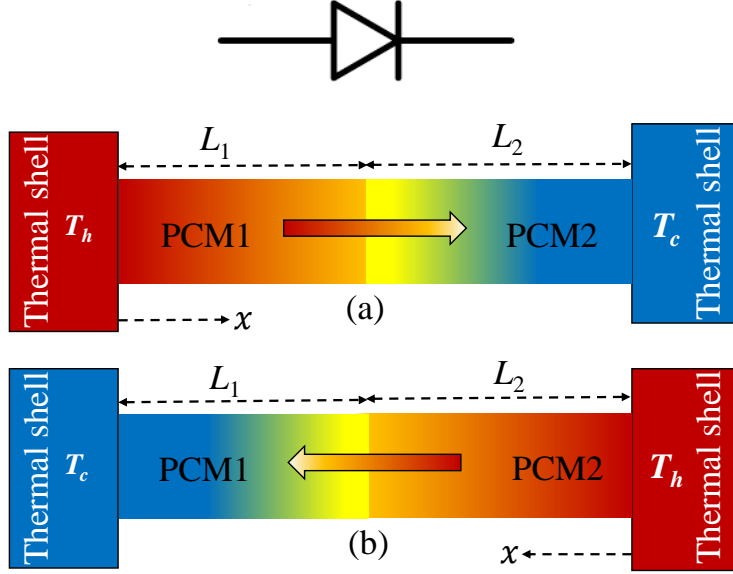


Figure 1: Scheme of a dual PCMs conductive thermal diode operating in the (a) forward and (b) backward configurations. Hot and cool thermal shells are set at the temperatures T_h and T_c , respectively.

2. THEORETICAL MODELING

Let us consider a system of two phase change materials exchanging heat through steady-state conduction as a result of their temperature difference $T_h - T_c > 0$, as illustrated in Figs. 1(a) and 1(b), respectively. In the forward configuration [Fig 1(a)], the heat flux q_F flows from PCM1 to PCM2, while in the backward one [Fig 1(b)], the heat flux q_B occurs in the opposite direction, as a result of the interchange of the temperatures T_h and T_c . The values of q_F and q_B are driven by the thermal conductivities of $\kappa_1(T)$ of PCM1 and $\kappa_2(T)$ of PCM2, and are not expected to be equal ($q_F \neq q_B$), due of the temperature dependence of $\kappa_1(T)$ and $\kappa_2(T)$. For temperatures within the MIT of VO_2 and PE. Therefore, the asymmetry of $\kappa_n(T)$ around its transition temperature T_{0n} , with $n = 1, 2$, is much larger. It allows optimizing the heat flux difference $q_F - q_B$ by setting the terminals' temperatures as follows: $T_c < T_{0n} < T_h$. The ability of this temperature-controlled thermal diode to rectify heat fluxes can thus be defined by the following rectification factor R [34]

$$R = \frac{|q_F - q_B|}{\max(q_F, q_B)}. \quad (1)$$

Equation (1) establishes that a nonzero rectification is achieved when the reversal of the temperature gradient induces not only the inversion of the heat flux direction, but also a significant variation of the heat flux magnitude. Optimal rectification ($R = 1$) is reached when one of the heat fluxes is zero.

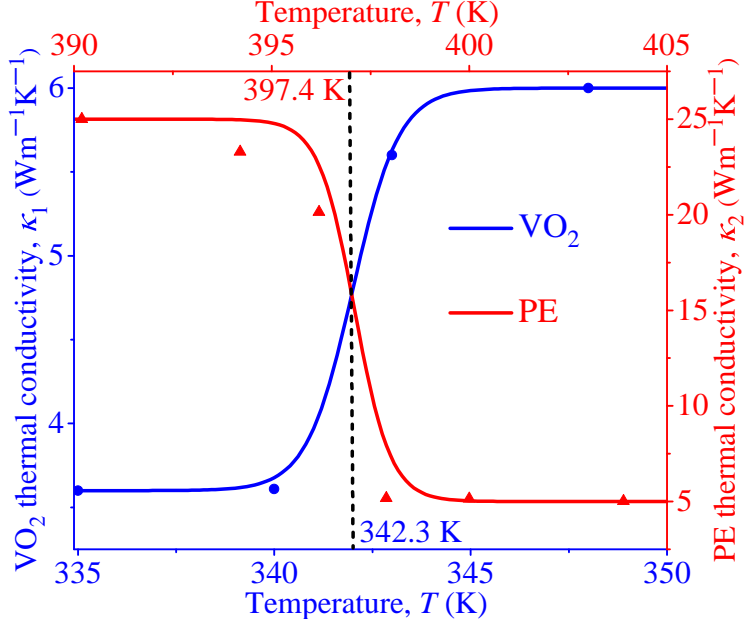


Figure 2: Thermal conductivities of VO₂ and PE, as functions of the temperature within their corresponding MIT. Dots and triangles stand for experimental data reported in the literature [37, 33], while lines represent the theoretical predictions of Eq. (3).

2.0.1. Forward configuration

According to the Fourier's law of heat conduction and the principle of energy conservation, the steady-state heat flux q_F in the forward configuration of the thermal diode shown in Fig 1(a), is given by

$$q_F = -\kappa_1(T_1) \frac{dT_1}{dx} = -\kappa_2(T_2) \frac{dT_2}{dx}, \quad (2)$$

where $T_1(x)$ and $T_2(x)$ are the temperatures within the PCM1 ($0 \leq x \leq L_1$) and PCM2 ($L_1 \leq x \leq L_1 + L_2$), respectively. In this work, we consider that the thermal conductivities $\kappa_1(T)$ and $\kappa_2(T)$ belong to VO₂ and PE, respectively, and their temperature variations are shown in Fig. 2, within their MITs. Note that the thermal conductivity contrast of PE ($25/5 = 5$) is higher than that of VO₂ ($6/3.6 = 1.7$), such that they reach their maximum thermal conductivities for temperatures $T < 395$ K and $T > 345$ K, respectively. This fact along with Eq. (2), indicates that q_F can be maximized by properly setting the temperatures T_h and T_c to fulfill these temperature conditions.

The thermal conductivities of both VO₂ and PE (Fig. 2) can be described by

$$\kappa_n(T) = \kappa_{in} + \frac{\kappa_{mn} - \kappa_{in}}{1 + e^{-\beta_n(T - T_{0n})}}, \quad (3)$$

where κ_{mn} and κ_{in} are the thermal conductivities in their respective high- and low-temperature phases, and β_n is the phase-transition slope of $\kappa_n(T)$ at the transition temperature $T = T_{0n}$, for $n = 1$ and 2. The

values of these four parameters were determined by fitting Eq. (3) to the experimental data shown in Fig. 2 for VO₂ and PE, and they are summarized in Table I.

Table 1: Material properties involved in Eqs. (3).

Material	$\kappa_{in}(\text{Wm}^{-1}\text{K}^{-1})$	$\kappa_{mn}(\text{Wm}^{-1}\text{K}^{-1})$	$\beta_n(\text{K}^{-1})$	$T_{0n}(\text{K})$
VO ₂	3.6	6	1.7	342.3
PE	25	5	2.2	397.4

The temperatures $T_1(x)$ and $T_2(x)$ can now be determined by integrating Eq. (2) for the thermal conductivities in Eq. (3), which yields

$$T_n(x) - T_{0n} + \frac{1}{\beta_n \gamma_n} \ln[1 + M_n(T_n(x))] = \frac{C_n}{\kappa_{mn}} - \frac{q_F}{\kappa_{mn}} x, \quad (4)$$

where C_n is an integration constant, $\gamma_n = \kappa_{mn}/(\kappa_{mn} - \kappa_{in})$, and $M_n(T) = \exp[-\beta_n(T - T_{0n})]$. The values of the three parameters q_F , C_1 and C_2 are determined by the boundary conditions $T_1(0) = T_h$, $T_2(L_1 + L_2) = T_c$, and $T_1(L_1) - T_2(L_1) = \rho q_F$, with ρ being the interface thermal resistance between the PCM1 and PCM2. Equation (4) thus yields the following expressions for the heat flux and temperature profiles

$$q_F = \frac{1}{\alpha_1} \ln \left[\frac{Z_1(T_h)}{Z_1(T_1(L_1))} \right], \quad (5a)$$

$$q_F = \frac{1}{\alpha_2} \ln \left[\frac{Z_2(T_1(L_1) - \rho q_F)}{Z_2(T_c)} \right], \quad (5b)$$

$$Z_1(T_1(x)) = [Z_1(T_h)]^{1-x/L_1} [Z_1(T_1(L_1))]^{x/L_1}, \quad (5c)$$

$$Z_2(T_2(x)) = [Z_2(T_1(L_1) - \rho q_F)]^{1-(x-L_1)/L_2} [Z_2(T_c)]^{(x-L_1)/L_2}, \quad (5d)$$

where $\alpha_n = \beta_n \gamma_n \rho_{mn}$, $\rho_{mn} = L_n/\kappa_{mn}$, and $Z_n(T) = [1 + M_n(T)] / [M_n(T)]^{\gamma_n}$. The substitution of Eq. (5a) into Eq. (5b) results in a strong non-linear dependence of the temperature $T_1(L_1) = \theta$ on T_h and T_c , as follows:

$$\left(\frac{Z_1(T_h)}{Z_1(\theta)} \right)^{\frac{\alpha_2}{\alpha_1}} = \frac{Z_2 \left(\theta - \frac{\rho}{\alpha_1} \ln \left[\frac{Z_1(T_h)}{Z_1(\theta)} \right] \right)}{Z_2(T_c)}. \quad (6)$$

After numerically solving Eq. (6) for the interface temperature θ , the forward heat flux and temperature profiles can be determined through Eqs. (5b)-(5d), for a given set of temperatures T_h and T_c .

2.0.2. Backward configuration

The backward heat flux (q_B) and the temperatures [$T_1(x)$ and $T_2(x)$] for the backward configuration [Fig. 1(b)], can be determined by following a similar approach than the one developed for the forward

configuration. The appropriate boundary conditions are $T_2(0) = T_h$, $T_1(L_1+L_2) = T_c$, and $T_2(L_2) - T_1(L_2) = \rho q_B$. The final results are

$$q_B = \frac{1}{\alpha_1} \ln \left[\frac{Z_1(T_1(L_2))}{Z_1(T_c)} \right], \quad (7a)$$

$$q_B = \frac{1}{\alpha_2} \ln \left[\frac{Z_2(T_h)}{Z_2(T_1(L_2) + \rho q_B)} \right], \quad (7b)$$

$$Z_1(T_1(x)) = [Z_1(T_1(L_2))]^{1-(x-L_2)/L_1} [Z_1(T_c)]^{(x-L_2)/L_1}, \quad (7c)$$

$$Z_2(T_2(x)) = [Z_2(T_h)]^{1-x/L_2} [Z_2(T_1(L_2) + \rho q_B)]^{x/L_2}. \quad (7d)$$

The combination of Eqs. (7a) and (7b) yields the following transcendental equation for the interface temperature $T_1(L_2) = \phi$, as a function of T_h and T_c :

$$\left(\frac{Z_1(\phi)}{Z_1(T_c)} \right)^{\frac{\alpha_2}{\alpha_1}} = \frac{Z_2(T_h)}{Z_2\left(\phi + \frac{\rho}{\alpha_1} \ln \left[\frac{Z_1(\phi)}{Z_1(T_c)} \right]\right)}. \quad (8)$$

The numerical solution of Eq. (8) for ϕ , fully describes the heat conduction in the thermal diode through Eqs. (7b)-(7d).

2.0.3. Rectification factor

In order to maximize q_F and minimize q_B for optimizing the rectification factor R in Eq. (1), we have conveniently rewrite Eqs. (5a), (5b), (7a), and (7b), as follows:

$$q_F = \frac{T_h - \theta}{\rho_{m1}} + \frac{(\rho_{m1})^{-1}}{\beta_1 \gamma_1} \ln \left[\frac{1 + e^{-\beta_1(T_h - T_{01})}}{1 + e^{-\beta_1(\theta - T_{01})}} \right], \quad (9a)$$

$$q_F = \frac{\theta - T_c}{\rho + \rho_{m2}} + \frac{(\rho + \rho_{m2})^{-1}}{\beta_2 \gamma_2} \ln \left[\frac{1 + e^{\beta_2(T_{02} + \rho q_F - \theta)}}{1 + e^{\beta_2(T_{02} - T_c)}} \right], \quad (9b)$$

$$q_B = \frac{\phi - T_c}{\rho_{m1}} - \frac{(\rho_{m1})^{-1}}{\beta_1 \gamma_1} \ln \left[\frac{1 + e^{\beta_1(T_{01} - T_c)}}{1 + e^{\beta_1(T_{01} - \phi)}} \right], \quad (9c)$$

$$q_B = \frac{T_h - \phi}{\rho + \rho_{m2}} - \frac{(\rho + \rho_{m2})^{-1}}{\beta_2 \gamma_2} \ln \left[\frac{1 + e^{-\beta_2(\phi - T_{02} + \rho q_B)}}{1 + e^{-\beta_2(T_h - T_{02})}} \right]. \quad (9d)$$

Equations (9a) and (9b) establishes that when the temperature T_h (T_c) is high (low) enough for fulfilling the conditions $\beta_1(T_h - T_{01}) \gg 1$, $\beta_1(\theta - T_{01}) \gg 1$, $\beta_2(T_{02} - T_c) \gg 1$, and $\beta_2(\rho q_F + T_{02} - \theta) \gg 1$, they reduce to

$$q_F = \frac{T_h - \theta}{\rho_{m1}} = \frac{\theta - T_c}{\rho + \rho_{i2}}, \quad (10)$$

where $\rho_{i2} = L_2/\kappa_{i2}$ and $\rho_{m1} = L_1/\kappa_{m1}$. Equation (10) explicitly indicates that, under these conditions, the whole terminal 1 (PCM1) is in its high-temperature (metallic) phase, while the entire terminal 2 (PCM2) is in its low-temperature one. According to Fig. 2, both of these phases are characterized by the highest thermal conductivities of PCM1 and PCM2, and therefore they maximize the heat flux $q_F = q_{F,\max}$ determined by

Eq. (10), as follows

$$q_{F,\max} = \frac{T_h - T_c}{\rho_{m1} + \rho + \rho_{i2}}, \quad (11a)$$

$$T_{1,\max}(L_1) = \frac{(\rho + \rho_{i2})T_h + \rho_{m1}T_c}{\rho_{m1} + \rho + \rho_{i2}}, \quad (11b)$$

$$T_{2,\max}(L_1) = \frac{\rho_{i2}T_h + (\rho_{m1} + \rho)T_c}{\rho_{m1} + \rho + \rho_{i2}}, \quad (11c)$$

where $T_1(L_1) = T_{1,\max}(L_1)$ and $T_2(L_1) = T_{2,\max}(L_1)$ are the interface temperatures associated to $q_{F,\max}$. On the other hand, Eqs. (9c) and (9d) show that when the temperature T_h (T_c) is high (low) enough for satisfying the conditions $\beta_1(T_{01} - T_c) \gg 1$, $\beta_1(T_{01} - \phi) \gg 1$, $\beta_2(T_h - T_{02}) \gg 1$, and $\beta_2(\rho q_B + \phi - T_{02}) \gg 1$, they turn into

$$q_B = \frac{\phi - T_c}{\rho_{i1}} = \frac{T_h - \phi}{\rho + \rho_{m2}}, \quad (12)$$

where $\rho_{i1} = L_1/\kappa_{i1}$ and $\rho_{m2} = L_2/\kappa_{m2}$. Equation (12) explicitly points out that, under these conditions, the whole terminal 1 (PCM1) is in its low-temperature (insulating) phase, while the entire terminal 2 (PCM2) is in its high-temperature one. According to Fig. 2, both of these phases correspond to the lowest thermal conductivities of PCM1 and PCM2, and hence they minimize the heat flux $q_B = q_{B,\min}$ given by Eq. (12), as follows

$$q_{B,\min} = \frac{T_h - T_c}{\rho_{i1} + \rho + \rho_{m2}}, \quad (13a)$$

$$T_{1,\min}(L_2) = \frac{\rho_{i1}T_h + (\rho + \rho_{m2})T_c}{\rho_{i1} + \rho + \rho_{m2}}, \quad (13b)$$

$$T_{2,\min}(L_2) = \frac{(\rho_{i1} + \rho)T_h + \rho_{m2}T_c}{\rho_{i1} + \rho + \rho_{m2}}, \quad (13c)$$

where $T_1(L_2) = T_{1,\min}(L_2)$ and $T_2(L_2) = T_{2,\min}(L_2)$ are the interface temperatures related to $q_B = q_{B,\min}$. According to Eqs. (1), (11a) and (13a), the optimal rectification factor $R_{\text{opt}} = 1 - q_{B,\min}/q_{F,\max}$ is then determined by

$$\begin{aligned} R_{\text{opt}} &= 1 - \frac{\rho_{m1} + \rho + \rho_{i2}}{\rho_{i1} + \rho + \rho_{m2}} \\ &= 1 - \frac{\kappa_{i1}}{\kappa_{m1}} \frac{(1 + \rho/\rho_{m1})r + \kappa_{m1}/\kappa_{i2}}{(1 + \rho/\rho_{i1})r + \kappa_{i1}/\kappa_{m2}}. \end{aligned} \quad (14)$$

where $r = L_1/L_2$. Note that R_{opt} is symmetric on the thermal resistances of both PCMs and increases with the thermal conductivity contrasts κ_{m1}/κ_{i1} and κ_{i2}/κ_{m2} between the metallic and insulator phases of the PCMs. In contrast to the optimal rectification factor of a conductive thermal diode operating with a single PCM [34], R_{opt} in Eq. (14) does depend on the interface thermal resistance ρ between the terminals, such that lower values of ρ yield higher values of R_{opt} . The optimization of the rectification factor of heterojunction based on two PCMs thus requires high values of κ_{m1}/κ_{i1} and κ_{i2}/κ_{m2} and low ones of ρ .

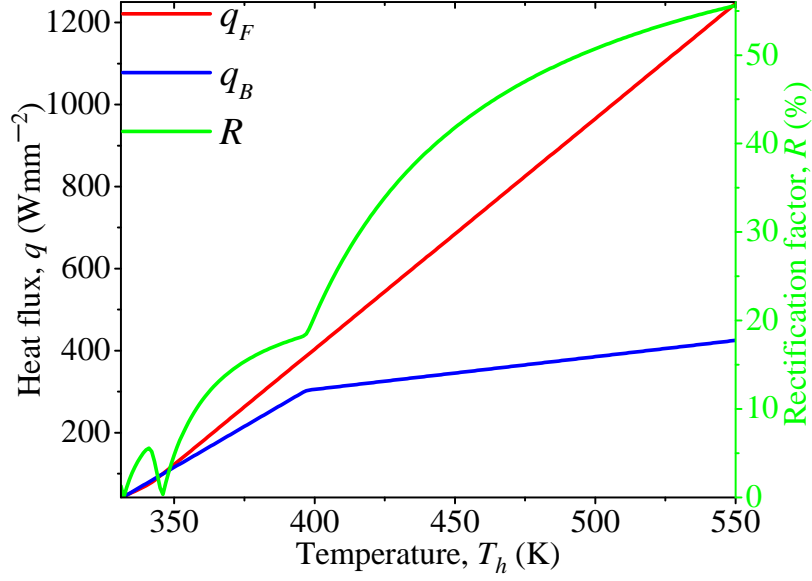


Figure 3: Rectification factor, forward and backward heat fluxes of the conductive thermal diode of VO₂ and PE, as functions of the temperature T_h . Calculations were done for $T_c = 300$ K and $\rho = 0 \text{ mm}^2\text{KW}^{-1}$.

3. RESULTS AND DISCUSSION

Figure 3 shows the temperature evolution of the forward (q_F) and backward (q_B) heat fluxes of a conductive thermal diode operating with terminals of VO₂ and PE. Note that both q_F and q_B exhibit a nearly linear increase with T_h , such that their difference is positive ($q_F - q_B > 0$), for most temperatures higher than the VO₂ transition one ($T_{01} = 342.5$ K). The slope change of q_F is due to the MIT transition of VO₂ at $T_h = T_{01}$, such that the difference $q_F - q_B$ increases for $T_h \gg T_{01}$. The heat fluxes q_F and q_B shown in Fig. 3 also increase with the interface temperatures $T_1(L_1)$ and $T_2(L_2)$, as shown in Figs. 4(a) and 4(b), respectively. This fact is consistent with Fig. 3, Eqs. (11a) and (13a) as well as with theoretical predictions [34, 38] and experimental data [35]. The metallic phase of VO₂ is thus able to enhance the rectification factor of the proposed conductive thermal diode when the temperature difference of its terminals is high enough.

The interface temperatures for the forward [$T_1(L_1)$ and $T_2(L_1)$] and backward [$T_2(L_2)$ and $T_1(L_2)$] configurations of the conductive thermal diode are respectively shown in Figs. 5(a) and 5(b), as functions of the temperature T_h . The expected increase of these four temperatures with T_h is driven by the combined effect of the thermal conductivities of VO₂ and PE, while the temperature differences $T_1(L_1) - T_2(L_1) = \rho q_F$ and $T_2(L_2) - T_1(L_2) = \rho q_B$ are determined by the forward and backward heat fluxes shown in Fig. 3, respectively. Larger interface temperature jumps are obtained for higher temperatures T_h , such as they tend to constant values (> 5 K) for $T_h > 380$ K. This fact along with Fig. 3, indicates that the optimization of the rectification factor of the conductive thermal diode requires relatively high temperature jumps at

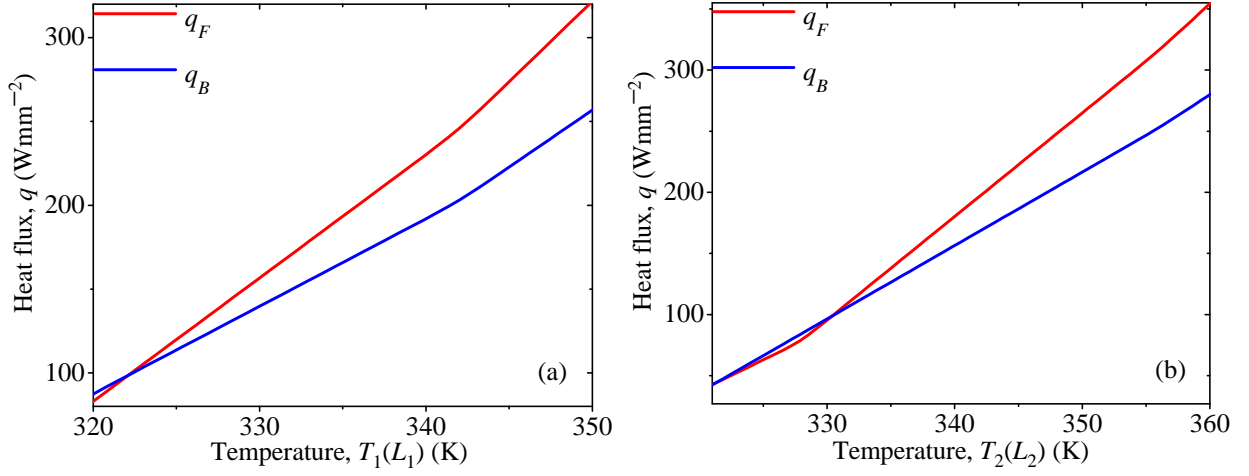


Figure 4: Temperature evolution of the forward and backward heat fluxes, as functions of (a) $T_1(L_1)$ and (b) $T_2(L_2)$. Calculations were done for $T_c = 300$ K and $\rho = 0$ mm²KW⁻¹.

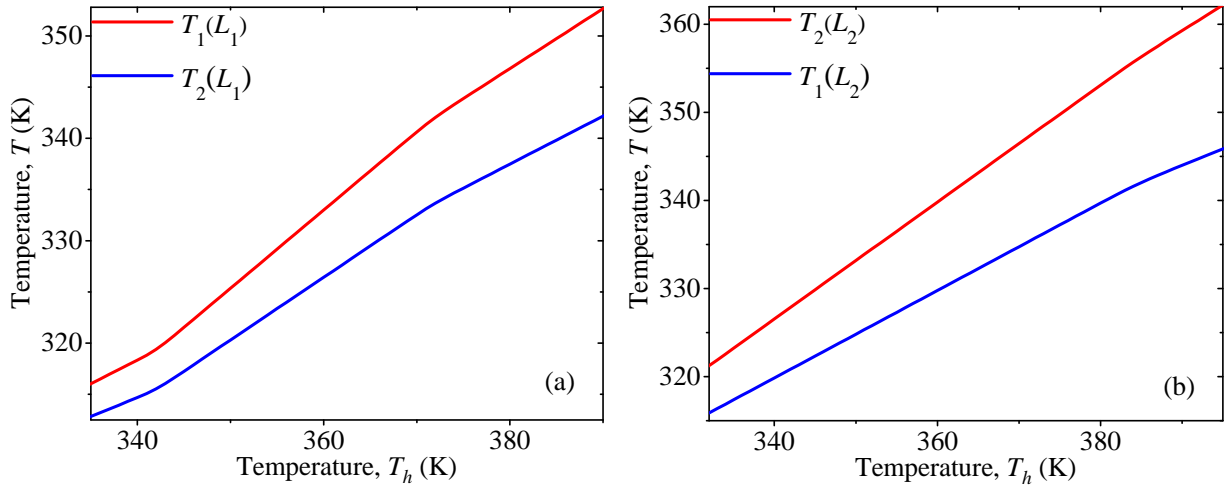


Figure 5: Interface temperatures for the (a) forward [$T_1(L_1)$ and $T_2(L_1)$] and (b) backward [$T_2(L_2)$ and $T_1(L_2)$] configurations, as functions of the temperature T_h . Calculations were done for $T_c = 300$ K and $\rho = 1$ mm²KW⁻¹.

the interface of its terminals, for a given interface thermal resistance $\rho > 0$. These jumps, of course, also increase with ρ and vanish for $\rho = 0$, as shown in Fig. 6. For a typical $\rho = 1$ mm²KW⁻¹, temperature jumps of $T_1(L_1) - T_2(L_1) = 65$ K and $T_2(L_2) - T_1(L_2) = 55$ K, are obtained for the forward and backward configurations, respectively. As the calculations in this latter figure were done for optimizing the rectification factor [$(T_h, T_c) = (550, 300)$ K], the almost linear behavior of the temperature within the PCM terminals is due to the fact that the terminals are either in their pure metallic or pure insulating phases. The slope change of the temperature at the interface $x = L_1$ is, therefore, as a result of the change of phase.

The rectification factor R of the proposed thermal diode is shown in Figs. 7, as a function of the

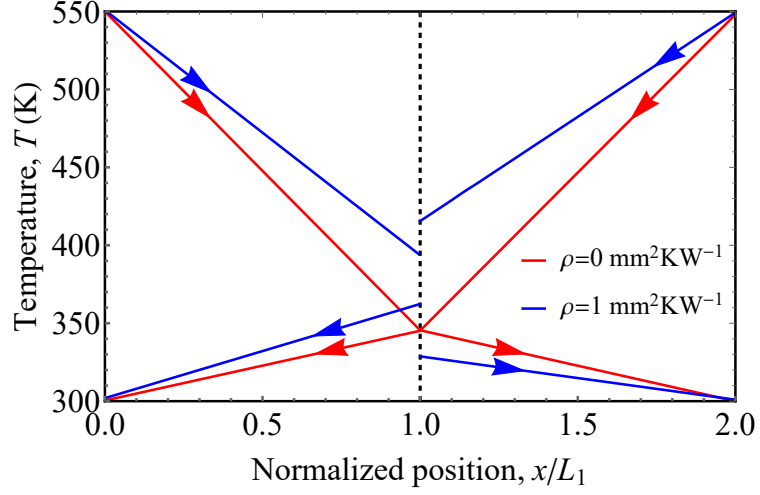


Figure 6: Temperature profiles within the terminals of the conductive thermal diode operating in the forward and backward configurations. Arrows stand for the direction of heat flux and calculations were done for $T_c = 300$ K, $T_h = 550$ K, and two values of the interface thermal resistance ρ .

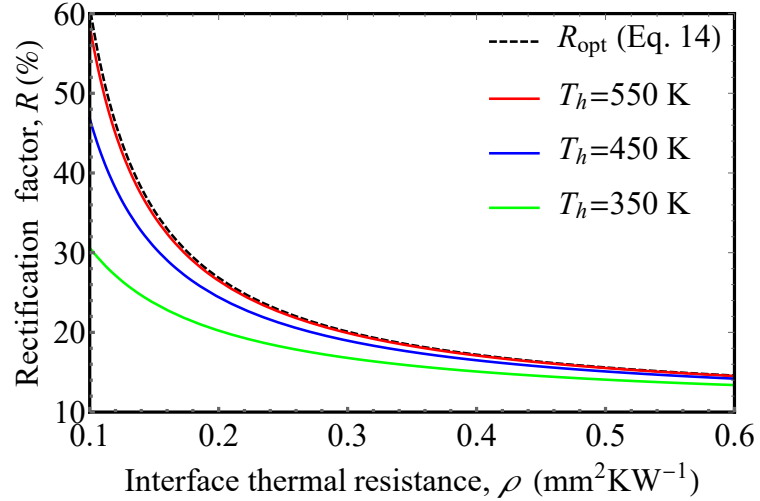


Figure 7: Rectification factor of the conductive thermal diode, as a function of the interface thermal resistance ρ . Calculations were done using $R = [1 - \min(q_F, q_B)/\max(q_F, q_B)]$ and $T_c = 300$ K.

interface thermal resistance ρ , for three values of the temperature T_h of the hotter terminal. Note that R increases as ρ decreases and/or T_h increases, such that its value for $T_h = 550$ K is well predicted by the analytical expression in Eq. (14). This verify the reliability of Eq. (14) to describe the optimal rectification factor, for different interface thermal resistance, and it indicates that the rectification factor reaches its maximum value for $T_h = 550$ K, as confirmed by the density plot in Fig. 8. Given that ρ is the interface thermal resistance between VO_2 and PE, its reduction to optimize the rectification factor will require careful control of the deposition parameters of the VO_2/PE heterojunction. The rectification factor

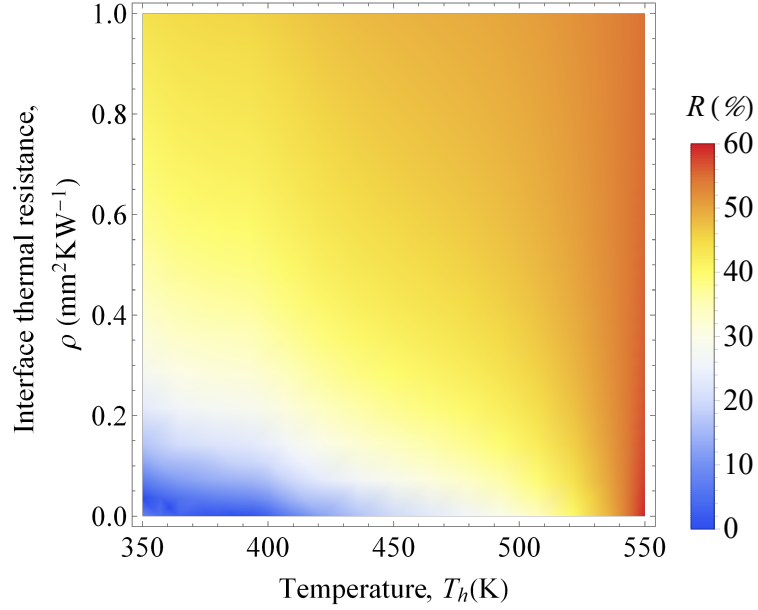


Figure 8: Density plot of the conductive thermal diode rectification factor as a function of the temperature T_h and interface thermal resistance ρ . Calculations were done using $R = [1 - \min(q_F, q_B)/\max(q_F, q_B)]$ and $T_c = 300$ K.

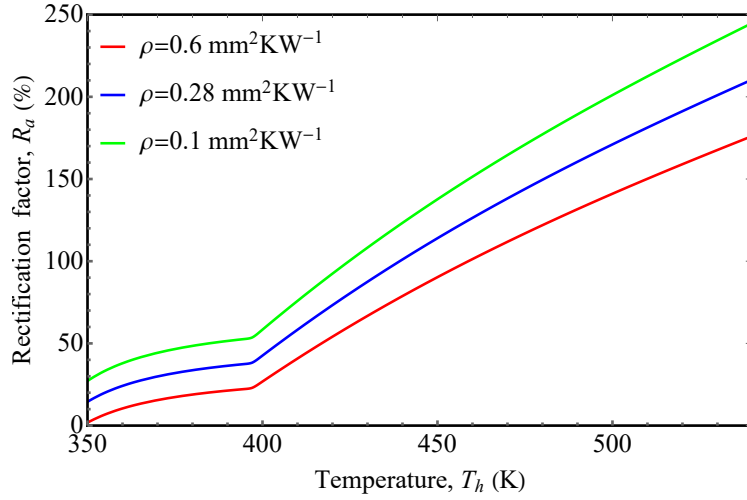


Figure 9: Rectification factor R of the conductive thermal diode as a function of the temperature T_h . Calculations were done by using the alternative definition $R_a = [\max(q_F, q_B)/\min(q_F, q_B)] - 1$ for three representative interface thermal resistances and $T_c = 300$ K.

at $T_h = 550$ K differs from the optimal one by only 3%, which reduces for higher values of T_h . The optimal rectification factor $R_{opt} = 60\%$ is reached for $\rho = 0 \text{ mm}^2\text{KW}^{-1}$ and a temperature difference of $T_h - T_c = 550 - 300 = 250$ K between the diode terminals. Similar temperature and thermal rectification factors have been reported for heterojunction made up of graphene-hexagonal boron nitride [39], graphene-graphene

phononic crystals [40], graphene nanoribbons [?] and carbon nanotube-graphene [41], but by involving temperatures relatively higher than the ones determined here for a VO₂/PE heterojunction. Furthermore, we note that the maximum rectification factor obtained for a conductive thermal diode operating with two (VO₂ and PE) PCMs is about 3 times the corresponding one obtained with a single PCM [34], which shows the advantage of properly combining the operation of two PCMs to enhance the thermal performance of conductive thermal diode. It is worth mentioning that in terms of the alternative definition of the rectification factor $R_a = [\max(q_F, q_B)/\min(q_F, q_B)] - 1$, the optimal rectification factor generated by the junction of VO₂ and PE is around 240%, which is greater than the 147% reported by Kang *et al.* [36]. This improvement is due to the difference in the thermal conductivity of tungsten-doped VO₂ used by Kang *et al.* [36] with respect to the one of pure VO₂ utilized in this work. This is reasonable, given that thermal diodes with higher rectification factors require larger thermal conductivity contrasts ($\kappa_{high}/\kappa_{low}$) for both of its terminals, as established by Eq. (14).

4. CONCLUSIONS

We have theoretically analyzed and optimized the rectification factor of a conductive thermal diode made up of a junction between two phase-change materials, whose thermal conductivities significantly change in a narrow interval of temperatures. This has been done by deriving analytical expressions for the temperature profiles, heat fluxes and rectification factor. A rectification factor up to 60% have been determined for a conductive thermal diode operating with terminals of VO₂ and polyethylene set with a temperature difference of 250 K from either side of the MIT temperatures. Higher rectification factors in a narrower temperature interval could be obtained with phase-change materials exhibiting higher thermal conductivity contrasts and faster phase transitions. The proposed model could thus be useful for guiding the development of phase-change materials capable of optimizing the rectification of conductive thermal diodes, which represent a fundamental building block for developing thermal circuits based on heat currents.

5. References

- [1] T.-M. Shih, Z. Gao, Z. Guo, H. Merlitz, P. J. Pagni, Z. Chen, Maximal rectification ratios for idealized bi-segment thermal rectifiers, *Sci. Rep.* 5 (2015) 12677.
- [2] N. Li, J. Ren, L. Wang, G. Zhang, P. Hänggi, B. Li, Colloquium: Phononics: Manipulating heat flow with electronic analogs and beyond, *Rev. Mod. Phys.* 84 (3) (2012) 1045.
- [3] N. A. Roberts, D. Walker, A review of thermal rectification observations and models in solid materials, *Int. J. Therm. Sci.* 50 (5) (2011) 648–662.
- [4] C. R. Otey, W. T. Lau, S. Fan, et al., Thermal rectification through vacuum, *Phys. Rev. Lett.* 104 (15) (2010) 154301.
- [5] H. Iizuka, S. Fan, Rectification of evanescent heat transfer between dielectric-coated and uncoated silicon carbide plates, *J. Appl. Phys.* 112 (2) (2012) 024304.

- [6] S. Basu, M. Francoeur, Near-field radiative transfer based thermal rectification using doped silicon, *Appl. Phys. Lett.* 98 (11) (2011) 113106.
- [7] L. Wang, Z. Zhang, Thermal rectification enabled by near-field radiative heat transfer between intrinsic silicon and a dissimilar material, *Nanosc. Microsc. Therm.* 17 (4) (2013) 337–348.
- [8] B. Li, L. Wang, G. Casati, Thermal diode: Rectification of heat flux, *Phys. Rev. Lett.* 93 (18) (2004) 184301.
- [9] K. Garcia-Garcia, J. Alvarez-Quintana, Thermal rectification assisted by lattice transitions, *Int. J. Therm. Sci.* 81 (2014) 76–83.
- [10] E. Pereira, Sufficient conditions for thermal rectification in general graded materials, *Phys. Rev. E* 83 (3) (2011) 031106.
- [11] G. Zhang, H. Zhang, Thermal conduction and rectification in few-layer graphene y junctions, *Nanoscale* 3 (11) (2011) 4604–4607.
- [12] D. Segal, Single mode heat rectifier: Controlling energy flow between electronic conductors, *Phys. Rev. Lett.* 100 (10) (2008) 105901.
- [13] L.-A. Wu, D. Segal, Sufficient conditions for thermal rectification in hybrid quantum structures, *Phys. Rev. Lett.* 102 (9) (2009) 095503.
- [14] J. Ordonez-Miranda, Y. Ezzahri, K. Joulain, Quantum thermal diode based on two interacting spinlike systems under different excitations, *Phys. Rev. E* 95 (2) (2017) 022128.
- [15] C. Starr, The copper oxide rectifier, *J. Appl. Phys.* 7 (1) (1936) 15–19.
- [16] G. Wu, B. Li, Thermal rectification in carbon nanotube intramolecular junctions: Molecular dynamics calculations, *Phys. Rev. B* 76 (8) (2007) 085424.
- [17] C. Chang, D. Okawa, A. Majumdar, A. Zettl, Solid-state thermal rectifier, *Science* 314 (5802) (2006) 1121–1124.
- [18] R. Scheibner, M. König, D. Reuter, A. Wieck, C. Gould, H. Buhmann, L. Molenkamp, Quantum dot as thermal rectifier, *New J. Phys.* 10 (8) (2008) 083016.
- [19] P. Van Zwol, L. Ranno, J. Chevrier, Tuning near field radiative heat flux through surface excitations with a metal insulator transition, *Phys. Rev. Lett.* 108 (23) (2012) 234301.
- [20] P. J. van Zwol, L. Ranno, J. Chevrier, Emissivity measurements with an atomic force microscope, *J. Appl. Phys.* 111 (6) (2012) 063110.
- [21] P. Van Zwol, K. Joulain, P. B. Abdallah, J.-J. Greffet, J. Chevrier, Fast nanoscale heat-flux modulation with phase-change materials, *Phys. Rev. B* 83 (20) (2011) 201404.
- [22] C. Tso, C. Y. Chao, Solid-state thermal diode with shape memory alloys, *Int. J. Heat Mass Transfer* 93 (2016) 605–611.
- [23] W. Kobayashi, Y. Teraoka, I. Terasaki, An oxide thermal rectifier, *Appl. Phys. Lett.* 95 (17) (2009) 171905.
- [24] N. Li, J. Ren, Non-reciprocal geometric wave diode by engineering asymmetric shapes of nonlinear materials, *Sci. Rep.* 4 (2014) 6228.
- [25] Y. Yang, H. Chen, H. Wang, N. Li, L. Zhang, Optimal thermal rectification of heterojunctions under fourier law, *Phys. Rev. E* 98 (4) (2018) 042131.
- [26] J. Ordonez-Miranda, Y. Ezzahri, J. Drevillon, K. Joulain, Transistorlike device for heating and cooling based on the thermal hysteresis of vo 2, *Phys. Rev. Appl.* 6 (5) (2016) 054003.
- [27] K. Ito, K. Nishikawa, H. Iizuka, H. Toshiyoshi, Experimental investigation of radiative thermal rectifier using vanadium dioxide, *Appl. Phys. Lett.* 105 (25) (2014) 253503.
- [28] M. Rini, Z. Hao, R. Schoenlein, C. Giannetti, F. Parmigiani, S. Fourmaux, J. Kieffer, A. Fujimori, M. Onoda, S. Wall, Optical switching in vo 2 films by below-gap excitation, *Appl. Phys. Lett.* 92 (18) (2008) 181904.
- [29] K. Ito, K. Nishikawa, H. Iizuka, Multilevel radiative thermal memory realized by the hysteretic metal-insulator transition of vanadium dioxide, *Appl. Phys. Lett.* 108 (5) (2016) 053507.
- [30] P. Ben-Abdallah, Thermal memristor and neuromorphic networks for manipulating heat flow, *AIP Adv.* 7 (6) (2017)

065002.

- [31] M. M. Qazilbash, Z. Li, V. Podzorov, M. Brehm, F. Keilmann, B. Chae, H.-T. Kim, D. Basov, Electrostatic modification of infrared response in gated structures based on VO_2 , *Appl. Phys. Lett.* 92 (24) (2008) 241906.
- [32] T. Driscoll, S. Palit, M. M. Qazilbash, M. Brehm, F. Keilmann, B.-G. Chae, S.-J. Yun, H.-T. Kim, S. Cho, N. M. Jokerst, et al., Dynamic tuning of an infrared hybrid-metamaterial resonance using vanadium dioxide, *Appl. Phys. Lett.* 93 (2) (2008) 024101.
- [33] T. Zhang, T. Luo, Giant thermal rectification from polyethylene nanofiber thermal diodes, *Small* 11 (36) (2015) 4657–4665.
- [34] J. Ordonez-Miranda, J. M. Hill, K. Joulain, Y. Ezzahri, J. Drevillon, Conductive thermal diode based on the thermal hysteresis of VO_2 and nitinol, *J. Appl. Phys.* 123 (8) (2018) 085102.
- [35] A. L. Cottrill, S. Wang, A. T. Liu, W.-J. Wang, M. S. Strano, Dual phase change thermal diodes for enhanced rectification ratios: Theory and experiment, *Adv. Energy Mater.* 8 (11) (2018) 1702692.
- [36] H. Kang, F. Yang, J. J. Urban, Thermal rectification via heterojunctions of solid-state phase-change materials, *Phys. Rev. Appl.* 10 (2) (2018) 024034.
- [37] D.-W. Oh, C. Ko, S. Ramanathan, D. G. Cahill, Thermal conductivity and dynamic heat capacity across the metal-insulator transition in thin film VO_2 , *Appl. Phys. Lett.* 96 (15) (2010) 151906.
- [38] W. Zhu, G. Wu, H. Chen, J. Ren, Nonlinear heat radiation induces thermal rectifier in asymmetric holey composites, *Front. Energy Res.* 6 (2018) 9.
- [39] X.-K. Chen, Z.-X. Xie, W.-X. Zhou, L.-M. Tang, K.-Q. Chen, Thermal rectification and negative differential thermal resistance behaviors in graphene/hexagonal boron nitride heterojunction, *Carbon* 100 (2016) 492–500.
- [40] S. Hu, M. An, N. Yang, B. Li, A series circuit of thermal rectifiers: an effective way to enhance rectification ratio, *Small* 13 (6) (2017) 1602726.
- [41] X. Yang, D. Yu, B. Cao, A. C. To, Ultrahigh thermal rectification in pillared graphene structure with carbon nanotube-graphene intramolecular junctions, *ACS Appl. Mater. Interfaces* 9 (1) (2016) 29–35.